Magnetic-Field-Calibration-Free Determination of the Hyperfine Constant A in Ultracold Fermi Gases of ^{40}K

Yajing Yang,[1,*] Biao Shan,[1,*] Yuhang Zhao,[1] Jiahui Shen,[1] Zhuxiong Ye,[1] Liangchao Chen,[1,2] Zengming Meng,[1,2] Pengjun Wang,[1,2] Wei Han,[1,2,†] Jing Zhang,[1,2,‡] and Lianghui Huang[1,2,§]

[1]*State Key Laboratory of Quantum Optics Technologies and Devices, Institute of Opto-electronics, Collaborative Innovation Center of Extreme Optics, Shanxi University, Taiyuan, Shanxi 030006, China*

[2]*Hefei National Laboratory, Hefei, Anhui 230088, China*

(Received 3 March 2026; revised 14 July 2026; accepted 1 September 2026; published 25 September 2026)

Hyperfine constant A is a key parameter of the hyperfine structure and underpins precision spectroscopy and metrology. In this Letter, we develop a magnetic-field-calibration-free method for determining the ground-state hyperfine constant A in an ultracold ^{40}K Fermi gas by utilizing a pair of magnetically insensitive ("clock") transitions. This overcomes the stringent magnetic-field calibration requirements of conventional methods. We measure the frequencies of these two magnetically insensitive transitions with Hz-level resolution over a range of magnetic fields and obtain the ground-state hyperfine constant $A = -h \times 285.730536(2)$ MHz, corresponding to an absolute uncertainty of about 2 Hz. Our value reduces the uncertainty by nearly 3 orders of magnitude compared with previous determinations, providing a substantially improved reference for high-precision spectroscopy and metrology with ^{40}K.

DOI: 10.1103/7sjf-yj2z

Fund Program for the Scientific Activities of Selected Returned Overseas Professionals in Shanxi ProvinceThe ground-state hyperfine structure constant A is the key atomic-structure parameter characterizing ground-state hyperfine splitting. With the development of atomic beam [1], atomic fountain [2], and optical frequency-comb techniques [3], ground-state hyperfine constants A of alkali isotopes such as $^{6/7}$Li [4], ^{23}Na [5], $^{39/41}$K [6,7], ^{85}Rb [8,9], ^{87}Rb [10], and ^{133}Cs [11,12] have been determined with extremely high accuracy so that the last significant digit typically corresponds to a frequency uncertainty better than the Hz level [13,14]. In particular, using atomic fountain and atomic beam resonance techniques, which operate on a magnetically insensitive clock transition under magnetic shielding and stringent magnetic-field calibration, the ground-state hyperfine splittings of ^{87}Rb and ^{133}Cs have been measured with uncertainties of a few μHz for ^{87}Rb [10] and about 0.1 Hz for ^{133}Cs [12], respectively.

However, not all alkali isotopes have reached this level of precision. For the fermionic isotope ^{40}K, traditional methods face significant difficulties in producing high-density atomic samples, primarily due to ^{40}K's extremely low natural abundance of only about 0.0117% [15,16]. Consequently, performing high-resolution absorption spectroscopy to determine the ground-state hyperfine constant A of ^{40}K is intrinsically challenging. The early measurement of A was determined using atomic beam spectroscopy at a high magnetic field and without magnetic shielding [17–19]. The corresponding value, $A = -h \times 285.7308(24)$ MHz, obtained from a later evaluation of those measurements [13], has been widely used in early studies of laser cooling, magneto-optical trapping, and degenerate Fermi gases [20–22]. However, with the development of ultracold atom experiments, its limited accuracy has now become a constraint. For example, it affects magnetic-field calibration, Feshbach-resonance fitting, and the extraction of spin-dependent interaction strengths, making magnetic-field scales difficult to compare across experiments and preventing further reduction of systematic uncertainties [23,24].

A more precise determination of the ground-state hyperfine constant A for ^{40}K is, therefore, crucial. In this Letter, we develop a magnetic-field-calibration-free experimental scheme for determining the ground-state hyperfine constant A through high-precision measurements of a pair of magnetically insensitive hyperfine transitions. Unlike conventional methods, this approach operates in an ultracold, quantum-degenerate regime in an optical trap, which greatly enhances the atomic density, and it exploits the magnetic-field insensitivity of the two transitions, thereby allowing the experiment to proceed without magnetic shielding and magnetic-field calibration. Using the developed method, we determined the ground-state hyperfine constant of ^{40}K to be $A = -h \times 285.730536(2)$ MHz with an absolute uncertainty of about 2 Hz, reducing the uncertainty by nearly 3 orders of magnitude compared with previous determinations [13,17–19].

*These authors contributed equally to this work.
†Contact author: hanwei.irain@gmail.com
‡Contact author: jzhang74@sxu.edu.cn
§Contact author: huanglh06@sxu.edu.cn

 © 2026 American Physical Society

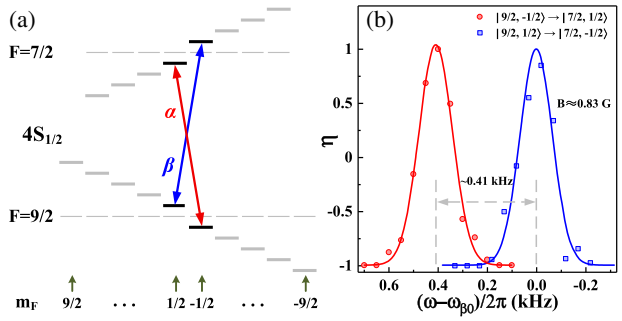

FIG. 1. (a) Energy-level diagram showing the single-photon microwave magnetically insensitive transitions α and β in ^{40}K. (b) Microwave spectra of the two sets of magnetically insensitive transitions α and β. The measurements are performed using a Gaussian-shaped π pulse with a duration of 10.5 ms and optimized amplitude under a bias magnetic field of 0.83 G. Here, $\omega_{\beta 0}$ denotes the resonance frequency for transition β.

We consider two magnetically insensitive single-photon transitions [25] labeled α for $|9/2,-1/2\rangle \Leftrightarrow |7/2,1/2\rangle$ and β for $|9/2,1/2\rangle \Leftrightarrow |7/2,-1/2\rangle$ within the ^{40}K ground-state hyperfine manifold, as shown in Fig. 1(a). In the presence of an external magnetic field B, the Zeeman energies of the hyperfine states depend on the magnetic quantum number m_F and are described by the Breit-Rabi formula [26,27],

$$E(B) = -\frac{A}{4} + \mu_B g_I m_F B \pm \frac{A(2I+1)}{4}\sqrt{1+\frac{4m_F}{2I+1}x+x^2}, \quad (1)$$

where $x = [2(g_J - g_I)\mu_B/A(2I+1)]B$, μ_B is the Bohr magneton, $+(-)$ refers to the energy levels in the ground-state hyperfine manifolds with $F = 9/2(7/2)$, and g_J and g_I are the Landé g factor of the electron and the nucleus, respectively [27]. Using Eq. (1), we obtain a set of coupled equations for the two transitions:

$$\begin{aligned}\omega_\alpha - \omega_\beta &= 2\mu_B g_I B/\hbar,\\ \omega_\alpha + \omega_\beta &= -\frac{A(2I+1)}{2\hbar}\left(\sqrt{1+\frac{2}{2I+1}x+x^2}\right.\\ &\quad \left.+\sqrt{1-\frac{2}{2I+1}x+x^2}\right),\end{aligned} \quad (2)$$

where $\omega_{\alpha/\beta}$ denotes the transition angular frequency. According to Eq. (2), one can find that the value of the magnetic field can be replaced by the frequency difference between the two transitions. Furthermore, we obtain an magnetic-field-calibration-free expression for the hyperfine constant A as

$$A = -2\hbar\omega_0\sqrt{\frac{1-M^2}{(2I+1)^2-M^2}}, \quad (3)$$

where $\omega_0 = (\omega_\alpha + \omega_\beta)/2$ and $M = (g_J - g_I/g_I)[\omega_\alpha - \omega_\beta/\omega_\alpha + \omega_\beta]$ (see Sec. I of Supplemental Material [28]).

A detailed description of the experimental setup is available in Refs. [40–45]. Initially, approximately $N = 4\times10^6$ ultracold ^{40}K atoms are prepared in the hyperfine Zeeman states $|9/2,-1/2\rangle$ and $|9/2,1/2\rangle$ for the α and β transitions, respectively, at a temperature of $0.3T_F$ in a crossed optical dipole trap (ODT), forming a deeply degenerate Fermi gas. Here the Fermi temperature is defined as $T_F = \hbar\bar{\omega}(6N)^{1/3}/k_B$, with $\bar{\omega}$ the geometric mean trapping frequency and k_B the Boltzmann constant [46]. Then the α and β transitions transfer atoms from the $F = 9/2$ manifold to $|7/2,1/2\rangle$ and $|7/2,-1/2\rangle$, respectively. To fully determine the populations of the initial and final states, an adiabatic Landau-Zener transition is used to transfer atoms from the $F = 7/2$ manifold back into a distinct Zeeman sublevel of the $F = 9/2$ manifold. By using time-of-flight absorption imaging with a Stern-Gerlach gradient magnetic field, we can simultaneously resolve the populations originating from both the initial and final states of the transitions. Finally, the transition frequencies are determined by locating the resonance condition, identified by the maximum of the population imbalance $\eta = (n_{7/2} - n_{9/2})/(n_{7/2} + n_{9/2})$, where n_F $(F = 7/2, 9/2)$ denotes the number of atoms in the respective Zeeman sublevel.

To measure the hyperfine constant A with high precision, we first perform microwave spectroscopy using a Gaussian-shaped π pulse to initially determine the two magnetically insensitive transition frequencies ω_α and ω_β [25], as shown in Fig. 1(b). We then determine these frequencies with much higher precision by employing Ramsey oscillations using two square microwave pulses of 0.15 ms duration, separated by a free-evolution time T_R (see Sec. II of Supplemental Material [28]). Because the transitions are approximately first-order magnetically insensitive, the transition frequency uncertainty is dominated by residual higher-order Zeeman shifts induced by magnetic-field noise. In our current experiment, with magnetic-field noise at approximately the 100 μG level, the Ramsey coherence time can reach several hundred milliseconds, as shown in Fig. 2, enabling Hertz-level frequency uncertainty. Moreover, a striking enhancement of coherence is observed as the magnetic field is reduced. At even lower magnetic fields, however, the coherence is instead limited by the near-degeneracy of hyperfine Zeeman sublevels and by state mixing induced by spin-exchange collisions [29]. By fitting the Ramsey fringes with a Gaussian phase-diffusion Ramsey model, we determine the transition angular frequency and the coherence time T_ϕ, where T_ϕ is defined as the Ramsey free-evolution time at which the rms accumulated phase uncertainty reaches one radian, i.e., $\sigma_\phi = \sigma_\omega T_\phi = 1$. The transition angular frequency uncertainty induced by magnetic field noise is then estimated as

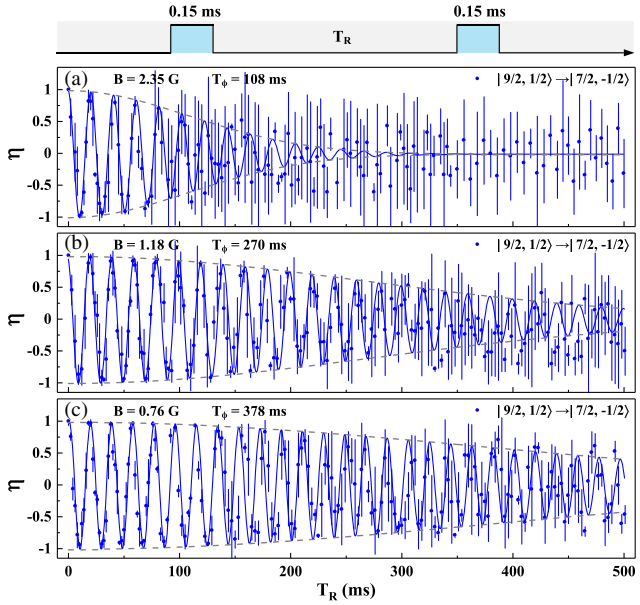

FIG. 2. Ramsey oscillations on the transition β as a function of the free-evolution time T_R at different bias magnetic fields, measured using a square $\pi/2$ pulse with duration $\tau_p = 0.15$ ms for state preparation and readout. The solid lines are fits using a Gaussian phase-diffusion model, while the dashed lines indicate the corresponding Ramsey contrast decay envelopes. Throughout this Letter, each data point represents the average of three independent measurements, and error bars denote one standard deviation.

$\sigma_\omega = 1/T_\phi$ (see Secs. III and V.A of Supplemental Material [28]).

Although ODTs offer the advantage of producing and maintaining high-density atomic samples over the entire interrogation time compared with traditional fountain clock methods, they also induce an ac Stark shift that affects the precise measurement of the transition frequencies [37,47]. In our experiment, the ODT is formed by far-detuned linearly polarized laser beams. In the low-intensity range, the dominant light shift arises from the second-order AC Stark effect and is, therefore, expected to scale linearly with optical intensity [36]. This allows us to extrapolate the resonance frequency to zero optical intensity via a linear fit, thereby effectively eliminating the trap-induced AC Stark frequency shift. In Fig. 3, we measure the light-induced shifts at different magnetic fields when the ODT intensity is varied and extrapolate them to zero intensity by linear fitting. The extrapolation uncertainty is mainly dominated by the covariance of the fitting procedure and the statistical uncertainties from repeated measurements at each data point (see Secs. IV.A and V.B of Supplemental Material [28]).

The use of a trapped degenerate Fermi gas is not expected to introduce a significant interaction-induced modification in the measured hyperfine constant A. This is because s-wave collisions are strongly suppressed by the Pauli exclusion principle, while interaction-induced shifts of the transition frequencies are absent due to the invariance of fermionic contact interactions under coherent driving [38,39]. Experimentally, this expectation is confirmed by the atomic density scan shown in Fig. 4, which shows no systematic dependence of the extracted hyperfine constant A on atomic density. The observed variations in A are limited to random fluctuations at the sub-Hz level, well below the measurement uncertainty (see Sec. V.C of Supplemental Material [28]). In addition, an accurate

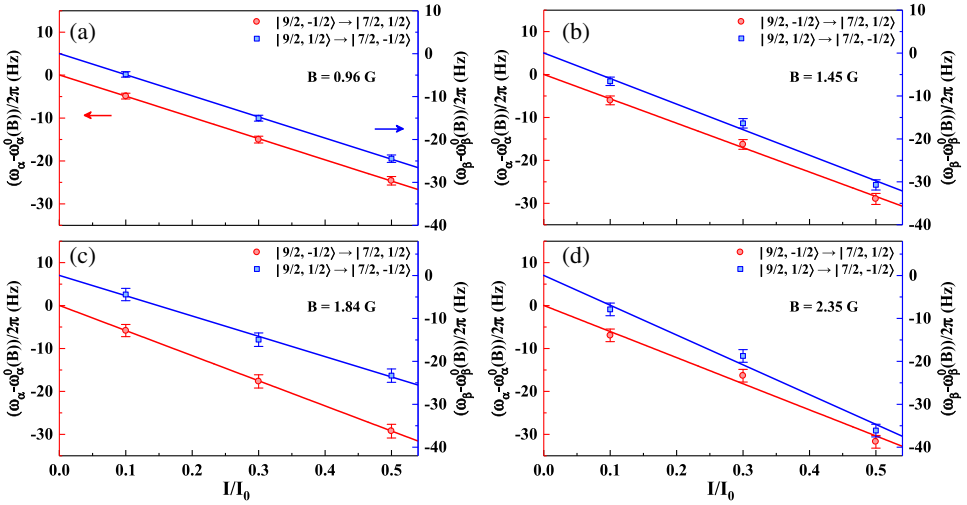

FIG. 3. Resonance frequencies of the α and β transitions versus ODT intensity at different bias magnetic fields. The α (β) data are plotted against the left (right) vertical axis. Here, $\omega_{\alpha(\beta)}$ denotes the resonance frequency at the given magnetic field and ODT intensity, and $\omega^0_{\alpha(\beta)}$ is the corresponding resonance frequency at $I = 0$ obtained by linear extrapolation. I_0 denotes the reference intensity at the center of the ODT formed by two mutually incoherent linearly polarized 1064 nm laser beams propagating in orthogonal directions, with powers of 3.5 and 2.5 W and waists of approximately 45 μm. Different trap intensities are obtained by proportional scaling of the laser powers at fixed beam waist.

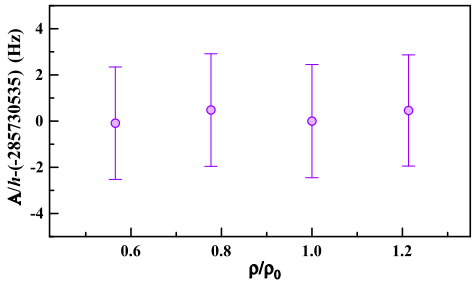

FIG. 4. Measured hyperfine constant A at different atomic densities. The bias magnetic field is fixed at $B = 1.06$ G and the ODT is maintained at $I = 0.1I_0$. $\rho_0 = 8 \times 10^{13}$ cm^{-3} denotes the reference density at the center of the ODT for $N = 4 \times 10^6$, while different densities are achieved by varying the atom number.

determination of the hyperfine constant A also depends on the precise experimental values of the Landé g factors g_J and g_I. At our current level of experimental precision, the available values of $g_J = 2.00229421(24)$ and $g_I = 0.000176490(34)$ [13,27] are sufficient for an accurate determination of A (see Sec. V.D of Supplemental Material [28]).

Finally, based on the measured frequencies of the two magnetically insensitive transitions, the hyperfine constant A can be determined according to Eq. (3), as shown in Fig. 5. It is found that the hyperfine constant A extracted at lower trap intensities exhibits greater stability against variations in the magnetic field, as illustrated in Fig. 5(a). Furthermore, a more precise value of A can be obtained by eliminating the trap-induced ac Stark shift via zero-intensity extrapolation, as shown in Fig. 5(b). Using the data in

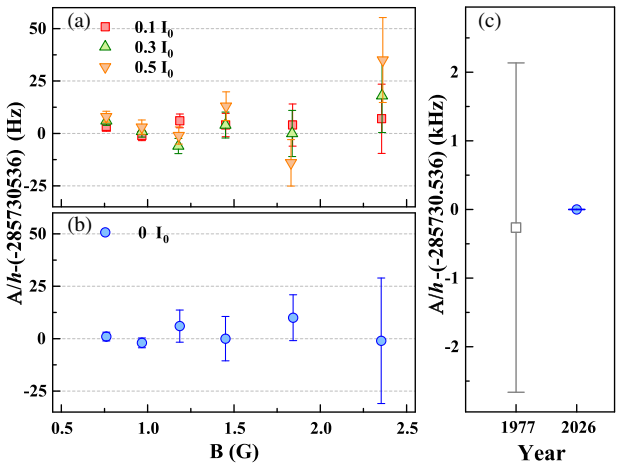

FIG. 5. (a) Measured hyperfine constant A at different magnetic fields and ODT intensities. (b) Measured hyperfine constant A after removing the ODT-induced ac Stark shift. (c) Hyperfine constant determined in this work compared with previous measurements reported in Refs. [13,17–19]. The gray square represents the previously recommended value $-h \times 285.7308(24)$ MHz in 1977 [13], while the blue dot shows the present value $A = -h \times 285.730536(2)$ MHz.

Fig. 5(b) and an inverse-variance weighted mean, the hyperfine structure constant of ^{40}K is determined to be $A = -h \times 285.730536(2)$ MHz. The 2 Hz uncertainty is obtained by accounting for contributions from magnetic-field noise, ac Stark shifts, and uncertainties in the Landé g factors, as well as the negligible interaction-induced shifts. Additional details on the precise determination and uncertainty budget of hyperfine constant A are provided in Secs. IV and V of Supplemental Material [28]. This value represents an improvement in precision of approximately 3 orders of magnitude over previously reported values [14], as presented in Fig. 5(c).

In conclusion, we develop a magnetic-field-calibration-free method to determine the hyperfine constant. The key idea is the simultaneous measurement of two specifically chosen magnetically insensitive transitions, from which the hyperfine constant can be directly extracted using only the measured transition frequencies. The magnetic-field insensitivity ensures Hertz-level precision in the frequency measurements. This enables the experiment to be performed without the magnetic shielding and magnetic-field calibration required in conventional methods. In contrast to conventional fountain clock and atomic beam approaches, we prepare a high-density ultracold atomic sample in the degenerate regime confined in an optical dipole trap, which significantly enhances the atomic density. Under these experimental conditions, we employ Ramsey interferometry to measure the two transition frequencies, leading to a determination of the hyperfine structure constant, $A = -h \times 285.730536(2)$ MHz. This result improves the most precise previously reported value by 3 orders of magnitude [13,17–19].

Our current work brings the measurement of the hyperfine constant of ^{40}K on the Hertz-level precision footing of other alkali-metal isotopes, thereby resolving a long-standing problem of low measurement precision for ^{40}K that has persisted for more than 70 years. The refined value of the hyperfine constant provides a more reliable atomic reference for precision spectroscopy, which can significantly improve applications in magnetic-field calibration [26,48], Feshbach-resonance fitting [24,49,50], and the determination of spin-dependent interaction strengths [51]. Moreover, this approach can be naturally extended to other atoms and hyperfine transitions that are important for quantum precision measurement and quantum sensing.

It should be noted that the two magnetically insensitive transitions employed in our scheme only eliminate the first-order differential Zeeman shift. The transition frequencies are still affected by higher-order Zeeman effects, which limit the atomic coherence time in Ramsey interferometry and make the measurements susceptible to magnetic-field noise, thereby confining the precision to the Hertz level. Further improvements, such as enhanced magnetic shielding and increased magnetic-field stability, could prolong the coherence time and enable the measurement precision

of the hyperfine constant to reach even higher levels. In the current experiment, the ODT-induced ac Stark shift is carefully characterized and compensated to minimize its impact on the measurements. In principle, the ac Stark shift is determined by the scalar, vector, and tensor polarizabilities of the atoms [37,47,52–55], which depend on the wavelength and polarization of the laser. In future experiments, by choosing an appropriate laser wavelength and polarization, it may be possible to eliminate the differential light shift of the clock transitions fundamentally.

Acknowledgments—This research is supported by the National Key Research and Development Program of China (Grants No. 2022YFA1404101 and No. 2021YFA1401700), Quantum Science and Technology-National Science and Technology Major Project (Grant No. 2021ZD0302003), National Natural Science Foundation of China (Grants No. 12034011, No. 92476001, No. U23A6004, No. 12488301, No. 12474266, No. 12474252, No. 12374245, No. 12322409, No. 92576205, and No. 12504336), the Fundamental Research Program of Shanxi Province (No. 202403021221001), and the Fund Program for the Scientific Activities of Selected Returned Overseas Professionals in Shanxi Province (No. 20250004).

Data availability—There are no publicly available research data or software supporting this manuscript. Requests for further information or data should be sent to the authors.

[1] N. F. Ramsey, *Molecular Beams* (Oxford University Press, New York, 1956).
[2] H. J. Metcalf and P. van der Straten, *Laser Cooling and Trapping of Neutral Atoms* (Springer-Verlag, New York, 1999).
[3] T. Udem, R. Holzwarth, and T. W. Hänsch, Optical frequency metrology, Nature (London) **416**, 233 (2002).
[4] R. G. Schlecht and D. W. McColm, Hyperfine structure of the stable lithium isotopes. I, Phys. Rev. **142**, 11 (1966).
[5] M. Arditi and T. R. Carver, Optical detection of zero-field hyperfine splitting of ^{23}Na, Phys. Rev. **109**, 1012 (1958).
[6] A. Beckmann, K. D. Böklen, and D. Elke, Precision measurements of the nuclear magnetic dipole moments of ^{6}Li, ^{7}Li, ^{23}Na, ^{39}K and ^{41}K, Z. Phys. **270**, 173 (1974).
[7] M. Peper, F. Helmrich, J. Butscher, J. A. Agner, H. Schmutz, F. Merkt, and J. Deiglmayr, Precision measurement of the ionization energy and quantum defects of ^{39}KI, Phys. Rev. A **100**, 012501 (2019).
[8] P. L. Bender, E. C. Beaty, and A. R. Chi, Optical detection of narrow ^{87}Rb hyperfine absorption lines, Phys. Rev. Lett. **1**, 311 (1958).
[9] Q. Wang, N. Zhang, W. Guang, S. Zhang, W. Wang, R. Wei, and Y. Wang, Precision measurements of the ground-state hyperfine splitting of ^{85}Rb using an atomic fountain clock, Phys. Rev. A **100**, 022510 (2019).
[10] Y. B. Ovchinnikov, K. Szymaniec, and S. Edris, Measurement of rubidium ground-state hyperfine transition frequency using atomic fountains, Metrologia **52**, 595 (2015).
[11] L. Essen and J. V. L. Parry, An atomic standard of frequency and time interval: A caesium resonator, Nature (London) **176**, 280 (1955).
[12] W. Markowitz, R. G. Hall, L. Essen, and J. V. L. Parry, Frequency of cesium in terms of ephemeris time, Phys. Rev. Lett. **1**, 105 (1958).
[13] E. Arimondo, M. Inguscio, and P. Violino, Experimental determinations of the hyperfine structure in the alkali atoms, Rev. Mod. Phys. **49**, 31 (1977).
[14] M. Allegrini, E. Arimondo, and L. A. Orozco, Survey of hyperfine structure measurements in alkali atoms, J. Phys. Chem. Ref. Data **51**, 043102 (2022).
[15] D. Wei, D.-Z. Xiong, H.-X. Chen, and J. Zhang, An enriched ^{40}K source for atomic cooling, Chin. Phys. Lett. **24**, 679 (2007).
[16] J. Meija, T. B. Coplen, M. Berglund, W. A. Brand, P. De Bièvre, M. Gröning, N. E. Holden, J. Irrgeher, R. D. Loss, T. Walczyk, and T. Prohaska, Isotopic compositions of the elements 2013 (IUPAC technical report), Pure Appl. Chem. **88**, 293 (2016).
[17] J. R. Zacharias, The nuclear spin and magnetic moment of K^{40}, Phys. Rev. **61**, 270 (1942).
[18] L. Davis, D. E. Nagle, and J. R. Zacharias, Atomic beam magnetic resonance experiments with radioactive elements Na^{22}, K^{40}, Cs^{135}, and Cs^{137}, Phys. Rev. **76**, 1068 (1949).
[19] J. T. Eisinger, B. Bederson, and B. T. Feld, The magnetic moment of K^{40} and the hyperfine structure anomaly of the potassium isotopes, Phys. Rev. **86**, 73 (1952).
[20] S. Falke, E. Tiemann, C. Lisdat, H. Schnatz, and G. Grosche, Transition frequencies of the D lines of ^{39}K, ^{40}K, and ^{41}K measured with a femtosecond laser frequency comb, Phys. Rev. A **74**, 032503 (2006).
[21] A. Behrle, M. Koschorreck, and M. Köhl, Isotope shift and hyperfine splitting of the $4s \rightarrow 5p$ transition in potassium, Phys. Rev. A **83**, 052507 (2011).
[22] R. K. Hanley, P. D. Gregory, I. G. Hughes, and S. L. Cornish, Absolute absorption on the potassium D lines: Theory and experiment, J. Phys. B: At. Mol. Opt. Phys. **48**, 195004 (2015).
[23] E. Wille, F. M. Spiegelhalder, G. Kerner, D. Naik, A. Trenkwalder, G. Hendl, F. Schreck, R. Grimm, T. G. Tiecke, J. T. M. Walraven, S. J. J. M. F. Kokkelmans, E. Tiesinga, and P. S. Julienne, Exploring an ultracold Fermi-Fermi mixture: Interspecies Feshbach resonances and scattering properties of ^{6}Li and ^{40}K, Phys. Rev. Lett. **100**, 053201 (2008).
[24] J. W. Park, C.-H. Wu, I. Santiago, T. G. Tiecke, P. Ahmadi, and M. W. Zwierlein, Quantum degenerate Bose-Fermi mixture of chemically different atomic species with widely tunable interactions, Phys. Rev. A **85**, 051602(R) (2012).
[25] B. Shan, L. Huang, Y. Yang, Y. Zhao, J. Shen, Z. Ye, L. Chen, Z. Meng, P. Wang, W. Han, and J. Zhang, Experimental study of magnetically insensitive transitions in an ultracold Fermi gas of ^{40}K, Phys. Rev. A **113**, 023306 (2026).

[26] G. Breit and I. I. Rabi, Measurement of nuclear spin, Phys. Rev. **38**, 2082 (1931).
[27] T. G. Tieckek, Properties of Potassium, https://tobiastiecke.nl/archive/PotassiumProperties.pdf (2019).
[28] See Supplemental Material at http://link.aps.org/supplemental/10.1103/7sjf-yj2z for a detailed description of the magnetic-field-calibration-free theoretical model, experimental details and microwave pulse generation, and the Ramsey measurement and fitting procedure, as well as the precise determination and uncertainty budget of the hyperfine constant A, which includes Refs. [13,25–27,29–39].
[29] P. Peng, L.-H. Huang, D.-H. Li, Z.-M. Meng, P.-J. Wang, and J. Zhang, Experimental observation of spin-exchange in ultracold Fermi gases, Chin. Phys. Lett. **35**, 033401 (2018).
[30] Z. Li, Z. Gu, Z. Shi, P. Wang, and J. Zhang, Quantum degenerate Bose-Fermi atomic gas mixture of ^{23}Na and ^{40}K, Chin. Phys. B **32**, 023701 (2023).
[31] T. M. Graham *et al.*, Multi-qubit entanglement and algorithms on a neutral-atom quantum computer, Nature (London) **604**, 457 (2022).
[32] V. Ivannikov and A. I. Sidorov, Phase diffusion in trapped-atom interferometers, J. Phys. B **51**, 205002 (2018).
[33] X.-T. Xu, Z.-Y. Wang, R.-H. Jiao, C.-R. Yi, W. Sun, and S. Chen, Ultra-low noise magnetic field for quantum gases, Rev. Sci. Instrum. **90**, 054708 (2019).
[34] C. Hölzl, A. Götzelmann, E. Pultinevicius, M. Wirth, and F. Meinert, Long-lived circular Rydberg qubits of alkaline-earth atoms in optical tweezers, Phys. Rev. X **14**, 021024 (2024).
[35] S. Tiengo, R. Eid, M. Apfel, G. Brulin, and T. Bourdel, A simple magnetic field stabilization technique for atomic Bose–Einstein condensate experiments, Rev. Sci. Instrum. **96**, 063201 (2025).
[36] D. A. Steck, Quantum and Atom Optics, https://steck.us/teaching (2022).
[37] J. Yang, X. He, R. Guo, P. Xu, K. Wang, C. Sheng, M. Liu, J. Wang, A. Derevianko, and M. Zhan, Coherence preservation of a single neutral atom qubit transferred between magic-intensity optical traps, Phys. Rev. Lett. **117**, 123201 (2016).
[38] S. Gupta, Z. Hadzibabic, M. W. Zwierlein, C. A. Stan, K. Dieckmann, C. H. Schunck, B. J. Verhaar, and W. Ketterle, Radio-frequency spectroscopy of ultracold fermions, Science **300**, 1723 (2003).
[39] M. W. Zwierlein, Z. Hadzibabic, S. Gupta, and W. Ketterle, Spectroscopic insensitivity to cold collisions in a two-state mixture of fermions, Phys. Rev. Lett. **91**, 250404 (2003).
[40] D. Wei, D. Xiong, H. Chen, P. Wang, L. Guo, and J. Zhang, Simultaneous magneto-optical trapping of fermionic ^{40}K and bosonic ^{87}Rb atoms, Chin. Phys. Lett. **24**, 1541 (2007).
[41] S. Chai, D. Wei, Z. Fu, L. Huang, and J. Zhang, The design of a dipole traps for Bose-Einstein condensate and degenerate Fermi gas, Acta Sin. Quantum Opt. **18**, 171 (2012).
[42] D. Wei, D. Xiong, H. Chen, and J. Zhang, A laser diode system for ^{40}K-^{87}Rb atomic cooling, Acta Phys. Sin. **55**, 6342 (2006).
[43] Y. Wang, L. Chen, P. Wang, and J. Zhang, The influence of gravitys effect on loading cold ^{87}Rb atoms into quadrupole magnetic trap, J. Opt. B **22**, 50 (2016).
[44] L. Chen, G. Yang, Z. Meng, L. Huang, P. Wang, and J. Zhang, Electromagnetically induced transparency in ^{87}Rb Bose-Einstein condensate, J. Opt. B **23**, 246 (2017).
[45] J. Miao, G. Bian, B. Shan, L. Chen, Z. Meng, P. Wang, L. Huang, and J. Zhang, Achieving ultracold Bose–Fermi mixture of ^{87}Rb and ^{40}K with dual dark magnetic-optical-trap, Chin. Phys. B **31**, 080306 (2022).
[46] P. Ding, B. Shan, Y. Zhao, Y. Yang, L. Chen, Z. Meng, P. Wang, L. Huang, and J. Zhang, Optimal preparation of Bose and Fermi atomic gas mixtures for ^{87}Rb and ^{40}K in a crossed optical dipole trap, Chin. Phys. B **33**, 063402 (2024).
[47] N. Lundblad, M. Schlosser, and J. V. Porto, Experimental observation of magic-wavelength behavior of ^{87}Rb atoms in an optical lattice, Phys. Rev. A **81**, 031611(R) (2010).
[48] C. A. Regal, M. Greiner, and D. S. Jin, Observation of resonance condensation of fermionic atom pairs, Phys. Rev. Lett. **92**, 040403 (2004).
[49] C. Chin, R. Grimm, P. S. Julienne, and E. Tiesinga, Feshbach resonances in ultracold gases, Rev. Mod. Phys. **82**, 1225 (2010).
[50] E. Wille, F. M. Spiegelhalder, G. Kerner, D. Naik, A. Trenkwalder, G. Hendl, F. Schreck, R. Grimm, T. G. Tiecke, J. T. M. Walraven, S. J. J. M. F. Kokkelmans, E. Tiesinga, and P. S. Julienne, Exploring an ultracold Fermi-Fermi mixture: Interspecies Feshbach resonances and scattering properties of ^{6}Li and ^{40}K, Phys. Rev. Lett. **100**, 053201 (2008).
[51] C. A. Regal and D. S. Jin, Measurement of positive and negative scattering lengths in a Fermi gas of atoms, Phys. Rev. Lett. **90**, 230404 (2003).
[52] J. Jiang and J. Mitroy, Hyperfine effects on potassium tune-out wavelengths and polarizabilities, Phys. Rev. A **88**, 032505 (2013).
[53] F. Schmidt, D. Mayer, M. Hohmann, T. Lausch, F. Kindermann, and A. Widera, Precision measurement of the ^{87}Rb tune-out wavelength in the hyperfine ground state $F = 1$ at 790 nm, Phys. Rev. A **93**, 022507 (2016).
[54] G. Li, Y. Tian, W. Wu, S. Li, X. Li, Y. Liu, P. Zhang, and T. Zhang, Triply magic conditions for microwave transition of optically trapped alkali-metal atoms, Phys. Rev. Lett. **123**, 253602 (2019).
[55] K. Wen, Z. Meng, L. Wang, L. Chen, L. Huang, P. Wang, and J. Zhang, Experimental study of tune-out wavelengths for spin-dependent optical lattice in ^{87}Rb Bose–Einstein condensation, J. Opt. Soc. Am. B **38**, 3269 (2021).